

# Performance of a Portable, Electromechanically-Cooled HPGe Detector for Site Characterization

Ronald M. Keyser and Richard C. Hagenauer  
ORTEC, 801 South Illinois Avenue, Oak Ridge, TN 37831

## 1 Introduction

High-resolution, germanium detectors (HPGe) have long been used for radionuclide characterization of nuclear sites, both buildings and large areas, for the purpose of cleaning up the site. Several systems consisting of a detector, mobile support, collimators and software for data collection and spectrum analysis have been made by national laboratories and commercial companies. The efficacy of these systems is well accepted. The use of HPGe detectors is complicated by the need for cryogenic cooling of the HPGe detector. The traditional method of cooling used liquid nitrogen and the handling of liquid nitrogen in field situations is always difficult. Laboratory type electromechanical coolers have been used for years, but only recently have developments in low-power electromechanical cooling for HPGe detectors made possible the construction of low weight, portable HPGe spectrometers with sufficient efficiency to perform the needed measurements in reasonable count times. The use of a battery-operated cooler simplifies the field operation by eliminating the need for transportation and storage of liquid nitrogen. The 12 volt DC power needed can be easily provided by AC adapter, additional battery packs, or automobile power.

For this work, the liquid nitrogen HPGe detector and MCA in a standard system for field measurements (Iso-Cart) was replaced by a portable HPGe detector with built-in MCA (Trans-SPEC-100). The detector is nominally 40% relative efficiency; a size commonly used for field measurements. The tungsten and steel collimators are cylindrical sleeves surrounding the crystal and projecting forward. The absorbing material is 4.7 mm thick.

The results show this detector performs well in this application and can be used to obtain reasonable detection limits in 1 hour counting times for both field (soil) and buildings (concrete). Details on the angular symmetry and efficiency as a



**Figure 1** Trans-SPEC-100 on Iso-Cart.

function of energy and distance are presented both with and without collimation.

## 2 Experimental

The system is shown in Fig. 1. The detector can be tilted at any angle for the best geometry for data collection, such as for walls or floors. It is not necessary to use low-background detectors because the natural activity in the field of view (FOV) is higher than the activity in the endcap material.

The field of view for large, flat surfaces for an uncollimated detector 1 meter above the ground was divided into zones by Beck<sup>1</sup>. The zones are shown in Fig. 2, with the percentages denoting the contribution to the spectrum from the ring of activity. Beck's work was extended to large HPGe detectors by Miller and Shebell<sup>2</sup>. The activity is assumed to be uniformly distributed. Note that more than 80% of the content of the spectrum comes from activity which is outside of the 1-meter diameter circle directly under the detector. The ability of the detector to collect the gamma rays from this area relies on the side efficiency of the detector. For measurements of small areas or areas surrounded by other materials, collimators are used to limit the FOV to the region of interest. Common paving materials have sufficient natural activity to reduce the ability to locate small spills by increasing the background.

The Trans-SPEC-100 detector efficiency is nominally 40% when measured according to IEEE 325, but this is for a point source at 25 cm in front of the detector. The Trans-SPEC-100 detector is nominally 6.5 cm diameter and 5 cm long. The detector will detect gamma rays on the front and sides, with some decrease at low energies on the sides due to the mounting cup (see Fig. 3), especially for a rugged detector designed to meet ANSI N42.34. Two

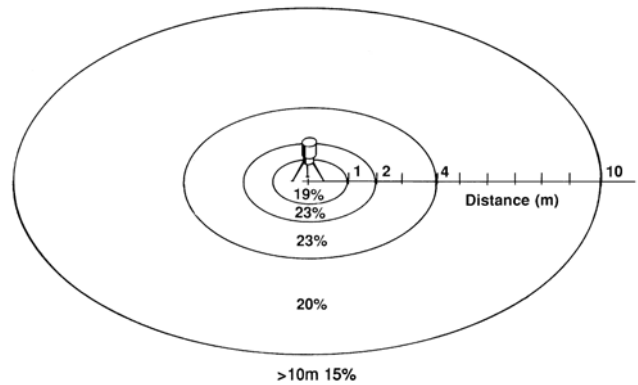


**Figure 2** FOV for 1-meter high detector.

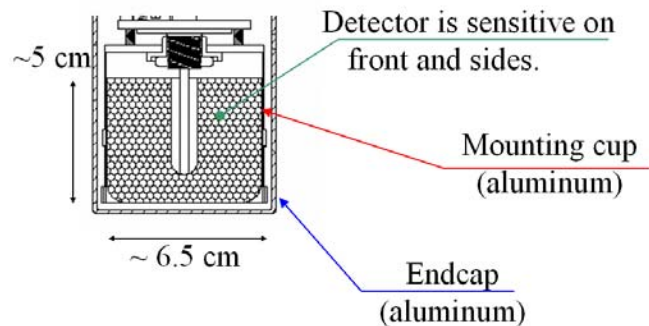


**Figure 3** Cross Section of HPGe Detector.

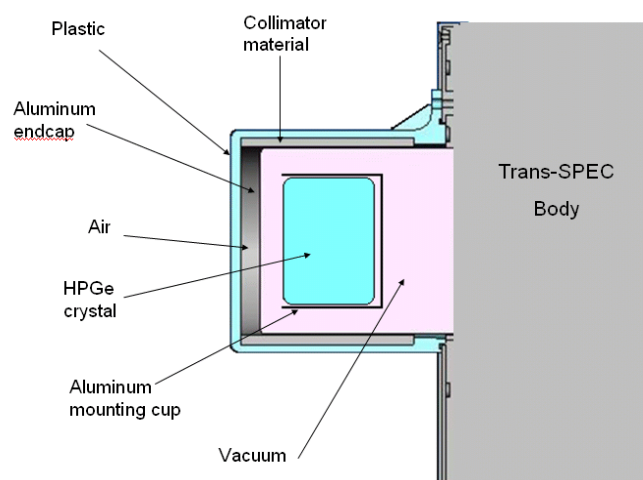


**Figure 4** Detector cross section showing collimator position.

different detectors were used for these measurements.

Figure 4 shows the detector with collimator. The metal part of the collimator is cast into the plastic mount. The plastic has some attenuation at low energies. The figure is nominally to scale. The collimator is 85 mm long and extends approximately 18 mm both forward and backward from the ends of the crystal. The collimator is 4.7 mm thick. Not shown are the mounting materials to the rear (toward the Trans-SPEC-100 body) of the crystal which provide additional shielding from that direction.

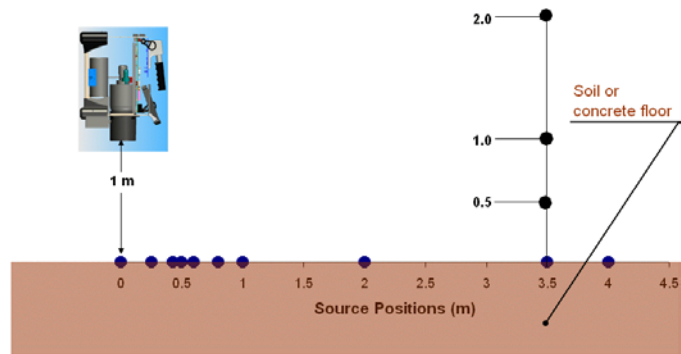


**Figure 5** Detector - Source Geometry.

The efficiency at different distances from the center point directly below the detector was measured in the geometries shown in Fig. 5. A multi-nuclide, NIST-traceable point source containing  $^{241}\text{Am}$ ,  $^{109}\text{Cd}$ ,  $^{57}\text{Co}$ ,  $^{139}\text{Ce}$ ,  $^{113}\text{Sn}$ ,  $^{137}\text{Cs}$ ,  $^{60}\text{Co}$ , and  $^{88}\text{Y}$  was placed at the positions shown, both horizontally and vertically at 3.5 meters distance. Spectra were recorded at each location with sufficient counts to minimize the impact of counting uncertainty.

In addition, the cylindrical symmetry was measured with the detector at 30 cm from the source and the same source placed 30 cm from the center horizontally and at  $0^\circ$ ,  $90^\circ$ ,  $180^\circ$ , and  $270^\circ$ . This geometry uses both the front face and the side area of the detector.

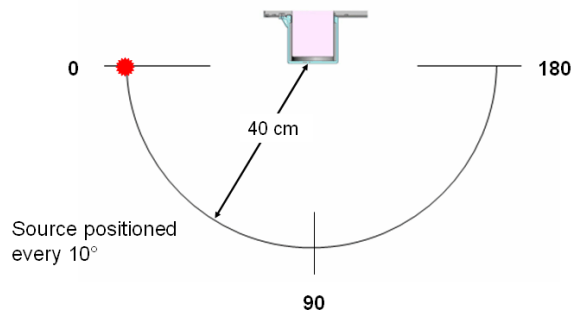


**Figure 6** Source positions around detector.

The efficiency at all points was calculated using GammaVision and the polynomial fit to the efficiency points. Peak areas were calculated by the summation method. Both 1461 keV ( $^{40}\text{K}$ ) and 2614 keV ( $^{208}\text{Tl}$ ) were assumed to be constant for all spectra and recorded to ensure quality of the spectra. The MDA values were calculated using the NuReg 4.16 formula.

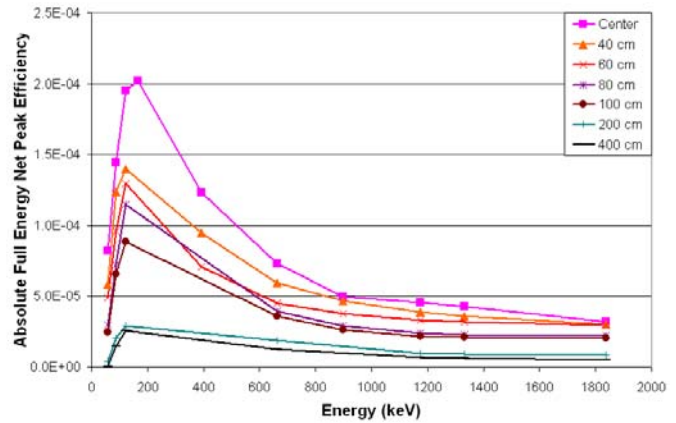
To measure the reduction of side-incident gamma rays using collimators, the source was positioned at 40 cm from the front of the collimator center point (about 41 cm from the detector endcap). The source ( $^{133}\text{Ba}$  or  $^{60}\text{Co}$ ) was positioned at  $10^\circ$  intervals around the center point. Spectra were collected for 1200 seconds in each point for the uncollimated, steel, and tungsten collimators. The peak areas for 81 (a doublet), 356, and 1332 keV were measured for each condition.

The 1-meter calculations are based on calculated efficiencies. For close geometries and collimated detectors the assumptions for this efficiency are not valid so the efficiency in activity calculations should be replaced with a measured efficiency. A geometry that represents the geometry of a small spill or other close-in counting is the 10 cm diameter

filter paper source positioned 10 cm from the endcap front. Two different mixed gamma ray emitting sources were used. The efficiencies were calculated using GammaVision and the polynomial fit.

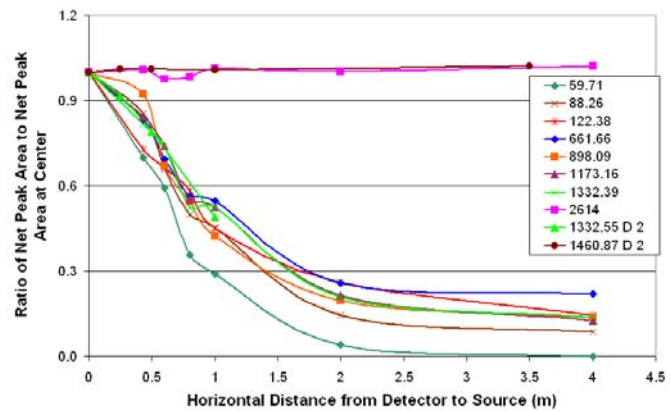
### 3 Results

The point source efficiency at each distance from the center point (as shown in Fig. 5) vs energy is shown in Fig. 7. The dependence on energy is typical for p-type detectors. Note that this is for a point source at the specified distance and is not weighted by the surface area shown in Fig. 2.



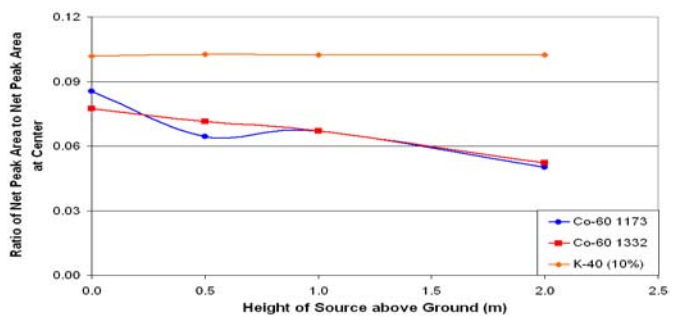
**Figure 7** Efficiency for Each Offset by Energy.

The efficiency can also be expressed as relative net peak count rate, where the count rate is normalized to the count rate at the center (or 0 distance). The plot of relative count rate at each energy vs distance is shown in Fig. 8. The reduction of efficiency with distance is somewhat expected. However, the lower energies are reduced more rapidly than the higher energies. This is due to absorption in the air. The 1460 and 2614 keV lines are also plotted. They are nominally constant as expected.



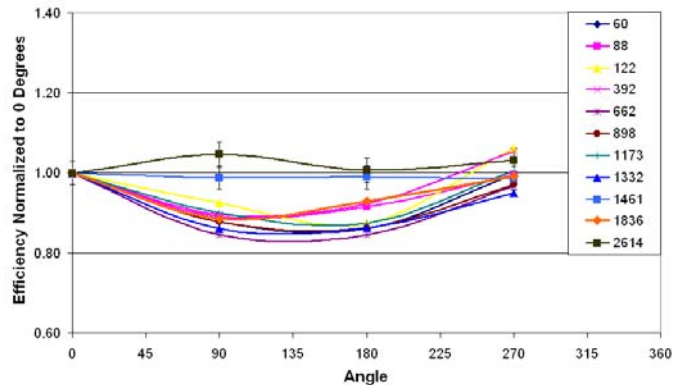
**Figure 8** Relative Net Peak Area vs Offset by Energy.

The net peak count rates of the higher energy gamma rays in Fig. 8 do not follow the inverse square dependence. It was suggested<sup>3</sup> that this was due to scattering from the ground. To test this, the source was counted in the vertical positions at 3.5 m distance as shown in Fig. 5. Figure 9 shows the relative net peak count rate as a function of source height. The reduction in count rate with increasing height would indicate the presence of scattering from the ground.



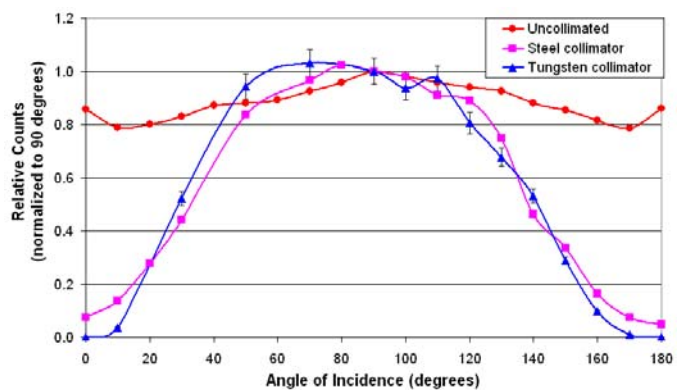
**Figure 9** Relative Net Peak Area vs Vertical Height at 3.5 m Distance.

Figure 10 shows the angular response of the detector. The 1461 and 2614 keV peak areas are relatively uniform as expected, but the source peak areas show a reduction in the 90 and 180 directions. This reduction is about 15% and can not be explained from the detector construction. The average data collection time was 7 hours.



**Figure 10** Relative Efficiency by Angle.

The collimator impact for 81 keV is shown in Fig. 11. The counts are normalized to the counts at 90°. The 81 keV lines are almost completely absorbed by either the steel or tungsten. The upturn in the uncollimated curve at 0° and 180° is due to the difference in absorption by the endcap, cup and germanium dead layer for the 0° angle of incidence and the 10° angle of incidence. The combined circular (front face) and cylindrical surface area of the detector perpendicular to the gamma ray flux has a maximum at about 45°, but this is reduced by the change in attenuation by the endcap and germanium dead layer with angle.



**Figure 11** Relative intensity of 81 keV peak vs angle of incidence for two different collimators and uncollimated.

Of more relevance is the 356 keV attenuation as shown in Fig. 12. The figure shows that the steel collimator reduces the side flux by 40% while the tungsten reduced it by more than 80% indicating that the tungsten collimator is more useful in the 100 to 500 keV range than steel.

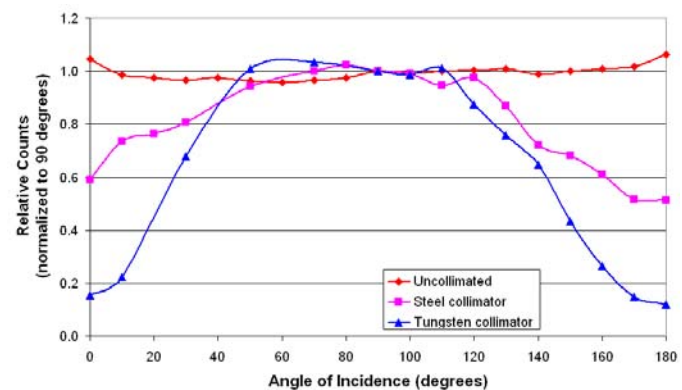


**Figure 12** Relative intensity of 356 keV peak vs angle of incidence for two different collimators and uncollimated.

The 1332 keV attenuation is shown in Fig. 13. The tungsten has a higher attenuation than steel (60% vs 70%), but for a significant reduction of 1460 keV ( $^{40}\text{K}$ ) or 2614 keV ( $^{208}\text{Tl}$ ), more tungsten should be used.

The absolute efficiency for the filter paper geometry is shown in Fig. 14. The maximum efficiency is about 0.011 at 140 keV. The region from 200 to 400 keV is not well fit because of a lack of un-interfered peaks with sufficient intensity in the region.

Using the point source efficiencies above, the MDA can be calculated for various nuclides using background counts from this detector. The background spectra from the soil (Tennessee) and the concrete floor of a building used in normal commerce were normalized to a count time of 1 hour and used to determine the MDA values shown in Table 1. The plutonium MDAs are high because of the low yield of gamma rays from  $^{239}\text{Pu}$ . The Trans-SPEC-100 detector is 65 mm diameter and 50 mm long. Also shown in Table 1 are the MDA values for a larger detector (80% relative efficiency<sup>4</sup>, 72 mm diameter and 87 mm long). As expected, the larger detector has lower MDA values for the same collection time.

The ratio of the MDAs (80% detector to Trans-SPEC-100) goes from 0.5 at low energies to 0.12 at high energies. The low-energy efficiency is proportional to the crystal surface area, while the high energy efficiency is proportional to the crystal volume, so these ratios are within expectations. This comparison is for unshielded detectors. Collimating the detectors will reduce the background and for small area measurements (such as spills) will reduce the advantage of the 80% over the 40%. The required detection limits vary with the purpose of the measurement (transportation, waste, or decontamination), country and regulatory agency, but the detection limits for the trans-SPEC-100 satisfy most decontamination (free release) limit requirements.

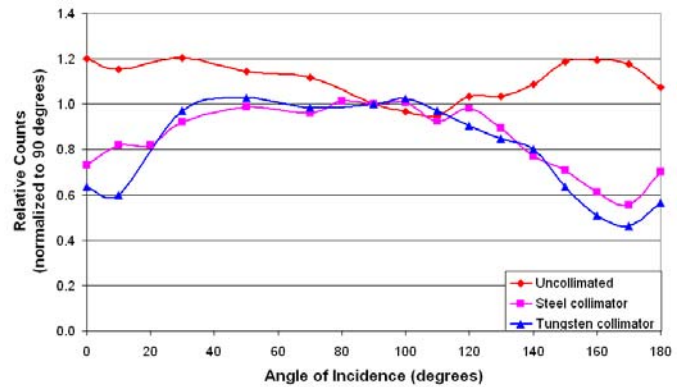


**Figure 13** Relative intensity of 1332 keV peak vs angle of incidence for two different collimators and uncollimated.

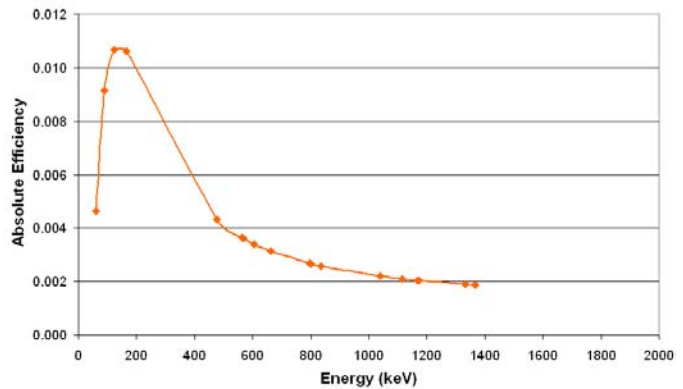


**Figure 14** Absolute Efficiency for 10 cm Disk Source at 10 cm Distance from Endcap.

<b>Table 1. MDA (Bq/m<sup>2</sup>) for Concrete Floor and Soil</b>				
		<b>Trans-SPEC-100</b>		<b>80%</b>
<b>Nuclide</b>	<b>Energy (keV)</b>	<b>Concrete Floor</b>	<b>Soil</b>	<b>Soil</b>
<b>Am-241</b>	<b>59.5</b>	<b>42</b>	<b>38</b>	<b>19</b>
<b>U-238</b>	<b>92.6</b>	<b>280</b>	<b>450</b>	<b>140</b>
<b>Pu-239</b>	<b>129.3</b>	<b>1.9E+05</b>	<b>3.9E+05</b>	<b>1.2E+05</b>
<b>U-235</b>	<b>185.7</b>	<b>25</b>	<b>34</b>	<b>9.7</b>
<b>Ba-133</b>	<b>355.0</b>	<b>19</b>	<b>31</b>	<b>6.6</b>
<b>Pu-239</b>	<b>413.7</b>	<b>8.0E+05</b>	<b>1.1E+06</b>	<b>2.7E+05</b>
<b>Cs-134</b>	<b>604.6</b>	<b>15</b>	<b>25</b>	<b>3.5</b>
<b>Cs-137</b>	<b>661.6</b>	<b>11</b>	<b>26</b>	<b>4.8</b>
<b>U-238</b>	<b>1001.1</b>	<b>970</b>	<b>1000</b>	<b>180</b>
<b>Co-60</b>	<b>1332.0</b>	<b>6.8</b>	<b>8.2</b>	<b>1.0</b>

#### 4 Conclusion

These data show that the detector in the Trans-SPEC-100 is suitable for use in field measurements and decommissioning of nuclear sites. The MDAs in the 1-meter mode satisfy most decontamination (free release) limit requirements. Thus, the advantage of using electromechanical cooling over liquid nitrogen cooling does not impose any disadvantage. The use of relatively low-weight collimators for characterizing small areas shows steel collimators can be used for energies below 120 keV, while tungsten should be used to reduce energies up to 800 keV. The measured efficiency for the extended source geometry shows good efficiency for use in counting containers at short distances. The complete system can be used site characterizations and spill measurements, especially in remote areas.

#### References

1. H. L. Beck, *et al*, In Situ Ge(Li) and NaI(Tl) Gamma-Ray Spectrometry, U.S. Department of Energy, Environmental Measurements Laboratory, HASL-258, September 1972.
2. K. M. Miller and P. Shebell, "Extension of a Generic Ge Detector Calibration Method for In Situ Gamma-Ray Spectrometry" *Radioactivity & Radiochemistry*, Vol. 11, pp. 14 - 24, December, 2000.
3. Richard Kouzes, Private communication.
4. Relative efficiency compared to 3" x 3" NaI detector as defined in IEEE 325.